

Explicit Asymptotic Performance Analysis of ESPRIT-Type Methods Exploiting the Difference Co-Array Concept

Zexiang Zhang[†], Qing Shen[†], Wei Liu[‡], Jiaming Yang[†], Chenxi Liao[†], Yizhe Wang[†]

[†]School of Information and Electronics, Beijing Institute of Technology, Beijing, China

[‡]Department of Electrical and Electronic Engineering, Hong Kong Polytechnic University, Kowloon, Hong Kong

Abstract—Over the past decade, the difference co-array (DCA) processing technique based on sparse arrays has attracted significant attention given its capability of addressing underdetermined direction-of-arrival (DOA) estimation problems. ESPRIT-type methods have been widely studied in this context; however, their closed-form asymptotic performance analysis for the underdetermined case remains an open problem. In this paper, the explicit asymptotic performance expression for the co-array-based standard ESPRIT method is first derived, followed by the derivation of closed-form performance bound for the co-array-based unitary ESPRIT (achieving reduced computational complexity compared to standard ESPRIT method). Simulation results confirm the tightness of derived performance bounds compared to the existing Cramér-Rao bound (CRB), providing an effective evaluation metric for both sparse array design and performance analysis.

Index Terms—Asymptotic performance analysis, ESPRIT, DOA estimation, sparse array, difference co-array

I. INTRODUCTION

Direction-of-arrival (DOA) estimation is a classical problem in applications such as radar, sonar, communication and navigation [1]. Subspace-based methods, exemplified by MUSIC [2], root-MUSIC [3], ESPRIT [4] and unitary ESPRIT [5], have been a long established approach to high resolution array signal processing.

However, for conventional processing methods, only $N - 1$ sources can be resolved by an N -sensor array structure. For the underdetermined DOA estimation case [6], which involves resolving more sources than the number of physical sensors, sparse arrays have been developed, with corresponding difference co-array (DCA) techniques proposed [7]–[9]. Over the past decade, the design of sparse arrays has witnessed significant progress [10]–[15]. By leveraging the *a priori* information that the sources are uncorrelated, a virtual array (referred to as the DCA) is generated by vectorizing the covariance matrix, providing $\mathcal{O}(N^2)$ degrees of freedom (DOFs) with only N physical sensors.

Although the compressive-sensing-based (CS-based) methods are capable of exploiting all DCA information, and thus achieving a relatively better estimation performance [6], [16], its large computational complexity limits its usage in real-time

practical applications; on the other hand, the complexity of co-array-based subspace methods is affordable. Compared with ESPRIT-type methods [4], [5], MUSIC-type methods [2], [3] exhibit superior performance but come with higher complexity, so overall the ESPRIT-type methods exhibit a balanced trade-off between performance and complexity.

In terms of performance analysis of the subspace-based methods, in [17], [18], a solid theoretical foundation for DOA estimation is established. Based on it, asymptotic performance analysis of MUSIC and ESPRIT exploiting the DCA concept were investigated in [19] and [20], respectively. However, the expressions given in [20] are derived from the “semi-algebraic” fashioned bias of virtual observation vector, where the closed-form expressions for fast performance evaluation of ESPRIT-type methods are still unknown.

In this paper, the asymptotic performance analysis for ESPRIT-type methods is presented. Firstly, we begin with a review of the standard ESPRIT and unitary ESPRIT methods exploiting the DCA concept. Then, a closed-form expression of the performance bound on DOA estimation of co-array-based standard ESPRIT method is derived. Finally, the unitary ESPRIT method is considered due to its further reduced complexity, and an explicit asymptotic performance bound is given. As verified by simulations, the derived performance bounds are sufficiently tight against experimental results, showing their effectiveness as evaluation tools.

II. SIGNAL MODEL

We consider a sparse linear array with N_p isotropic sensors placed at $\{l_n d\}_{n=1}^{N_p}$, where $l_n d$ denotes the position of the n -th sensor and $d \leq \frac{\lambda}{2}$ is the unit inter-element spacing with λ being the signal wavelength. $\mathbf{l} = [l_1 d, \dots, l_{N_p} d]^T$ is a vector consisting of all sensor positions.

K far-field uncorrelated narrowband sources, modeled as i.i.d. circularly symmetric complex Gaussian, are considered to impinge from directions $\theta_k \in (-90^\circ, 90^\circ)$. The corresponding source signals are $\{s_k(t)\}_{k=1}^K$, each with power $\{p_k\}_{k=1}^K$. The array output can be expressed as

$$\mathbf{x}(t) = \mathbf{A}\mathbf{s}(t) + \mathbf{n}(t), \quad (1)$$

where $\mathbf{x}(t)$ is the observed signal vector, $\mathbf{s}(t)$ is the source signal vector, and $\mathbf{n}(t)$ is the zero-mean additive white

This work was supported by the National Natural Science Foundation of China under Grant 62271052.

Gaussian noise vector with power σ_n^2 . The steering matrix $\mathbf{A} = \exp(-j\frac{2\pi}{\lambda}\mathbf{l}\mathbf{u}) \in \mathbb{C}^{N_p \times K}$, where the source directional vector is defined as $\mathbf{u} = [\sin \theta_1, \dots, \sin \theta_K]$.

The covariance matrix of the observed data is

$$\mathbf{R} = \mathbb{E}[\mathbf{x}(t)\mathbf{x}^H(t)] = \mathbf{A}\mathbf{P}\mathbf{A}^H + \sigma_n^2\mathbf{I}_{N_p}, \quad (2)$$

where $\mathbf{P} = \text{diag}([p_1, \dots, p_K]) \in \mathbb{C}^{K \times K}$ is the source signal covariance matrix, and \mathbf{I}_{N_p} is an identity matrix. Vectorizing \mathbf{R} leads to $\mathbf{r} = (\mathbf{A}^* \odot \mathbf{A})\mathbf{p} + \sigma_n^2\mathbf{i}$, where \odot denotes Khatri-Rao product, $\mathbf{p} = [p_1, \dots, p_K]^T$, and $\mathbf{i} = \text{vec}(\mathbf{I}_{N_p})$. After merging the repeated entries [16], we obtain

$$\mathbf{r}_1 = \mathbf{F}\mathbf{r} = \mathbf{A}_v\mathbf{p} + \sigma_n^2\mathbf{F}\mathbf{i} \in \mathbb{C}^{N_v \times 1}, \quad (3)$$

where $\mathbf{F} \in \mathbb{R}^{N_v \times N_p^2}$ is the selection matrix defined in [19]. N_v is the number of consecutive virtual sensors in the DCA, and the i_1 -th row vector of the selection matrix is

$$\mathbf{f}_{(i_1,:)} = \{\text{vec}[\mathbf{F}(i_1)]\}^T. \quad (4)$$

The (i_2, i_3) element in $\mathbf{F}(i_1) \in \mathbb{R}^{N_p \times N_p}$ can be expressed as

$$F(i_1)_{(i_2, i_3)} = \begin{cases} \frac{1}{w(i_1)}, & l_{i_2} - l_{i_3} = l_{v(i_1)}, \\ 0, & \text{otherwise,} \end{cases} \quad (5)$$

where $l_{v(i_1)}$, l_{i_2} , and l_{i_3} are the i_1 -th element in the consecutive segment of the DCA, the i_2 -th and i_3 -th element in the sensor position vector \mathbf{l} , respectively. $w(i_1)$ is the weight function defined as

$$w(i_1) = |\{(i_2, i_3) \mid l_{i_2} - l_{i_3} = l_{v(i_1)}\}|, \quad (6)$$

where $|\cdot|$ returns the cardinality of the input set. \mathbf{A}_v behaves as the manifold of a large virtual array corresponding to DCA.

The virtual array model consists of only a single snapshot, and the spatial smoothing (SS) technique is employed to recover the rank of virtual source covariance matrix by dividing the physical array into subarrays, and then followed by an averaging process. Denote \bar{N}_v as the number of subarray sensors. The number of subarrays is $N_{SS} = N_v - \bar{N}_v + 1$. The SS matrix $\mathbf{\Gamma}$ is

$$\mathbf{\Gamma} = [\mathbf{\Gamma}_1^T, \dots, \mathbf{\Gamma}_{N_{SS}}^T]^T, \quad (7)$$

where

$$\mathbf{\Gamma}_i = [\mathbf{0}_{\bar{N}_v \times (i-1)}, \mathbf{I}_{\bar{N}_v}, \mathbf{0}_{\bar{N}_v \times (N_{SS}-i)}]. \quad (8)$$

Without loss of generality, we set $\bar{N}_v = N_{SS}$, and the virtual observation data matrix of DCA can be obtained via matricization as

$$\mathbf{X}_v = \text{mat}_{\bar{N}_v, \bar{N}_v}(\mathbf{\Gamma}\mathbf{F}\mathbf{r}) = \mathbf{A}_v\mathbf{P}\mathbf{A}_v^H + \sigma_n^2\mathbf{I}. \quad (9)$$

Here, \mathbf{A}_v is the steering matrix of each subarray by choosing its first sensor as the reference, i.e., $\mathbf{A}_v = \exp(-j\frac{2\pi}{\lambda}\bar{\mathbf{l}}_v\mathbf{u})$ with $\bar{\mathbf{l}}_v = [0, \dots, \bar{N}_v - 1]^T d$. $\mathbf{A} = \text{mat}_{a,b}(\mathbf{a})$ denotes the reshaping operator that maps a vector $\mathbf{a} \in \mathbb{C}^{ab \times 1}$ to a matrix $\mathbf{A} \in \mathbb{C}^{a \times b}$. The well-known ESPRIT-type methods can be applied to \mathbf{X}_v for DOA estimation [20], [21].

III. EXPLICIT MSE EXPRESSION OF CO-ARRAY-BASED ESPRIT-TYPE METHODS

In the following part, we derive an explicit expression for the mean squared error (MSE) of the DCA-based standard ESPRIT and unitary ESPRIT methods.

A. Performance Analysis of Co-Array-Based Standard ESPRIT

Denote $\mathbf{X}_{v_0} = \mathbf{A}_v\mathbf{P}\mathbf{A}_v^H$ as the noise-free version of the virtual observation matrix. Performing the singular value decomposition (SVD) leads to

$$\mathbf{X}_{v_0} = \mathbf{U}_s\mathbf{\Sigma}_s\mathbf{U}_s^H + \mathbf{U}_n\mathbf{\Sigma}_n\mathbf{U}_n^H, \quad (10)$$

where \mathbf{U}_s and \mathbf{U}_n are the signal and noise subspaces in the noise-free case, respectively, while $\mathbf{\Sigma}_s$ and $\mathbf{\Sigma}_n$ are diagonal matrices holding larger K singular values and the rest singular values, respectively. Denote $\hat{\mathbf{U}}_s = \mathbf{U}_s + \Delta\mathbf{U}_s$ as the estimation of signal subspace under the noisy situation. According to [17], [20], we have

$$\Delta\mathbf{U}_s = \mathbf{U}_n\mathbf{U}_n^H\Delta\mathbf{X}_v\mathbf{U}_s\mathbf{\Sigma}_s^{-1}, \quad (11)$$

where $\Delta\mathbf{X}_v$ is the perturbation of \mathbf{X}_v in (9). The signal subspace \mathbf{U}_s is used to form the rotation invariance equation $\mathbf{J}_1\mathbf{U}_s\mathbf{\Psi} = \mathbf{J}_2\mathbf{U}_s$ with $\mathbf{\Psi} = \mathbf{T}\mathbf{\Phi}\mathbf{T}^{-1}$, where $\mathbf{J}_1 = [\mathbf{I}_{\bar{N}_v-1}, \mathbf{0}_{\bar{N}_v-1}]$ and $\mathbf{J}_2 = [\mathbf{0}_{\bar{N}_v-1}, \mathbf{I}_{\bar{N}_v-1}]$ serve as subarray selection matrices. $\mathbf{\Phi} = \text{diag}([\mu_1, \dots, \mu_K])$ contains the DOA information with $\mu_k = \exp(-j\frac{2\pi}{\lambda}d \sin \theta_k)$. We use \mathbf{p}_k^T to represent the k -th row in \mathbf{T}^{-1} , and \mathbf{q}_k denotes the k -th column in \mathbf{T} . The estimation error of the eigenvalue of the rotation invariance matrix is given by [17]

$$\Delta\mu_k = \mathbf{p}_k^T(\mathbf{J}_1\mathbf{U}_s)^\dagger(\mathbf{J}_2 - \mu_k\mathbf{J}_1)\mathbf{U}_n\mathbf{U}_n^H\Delta\mathbf{X}_v\mathbf{U}_s\mathbf{\Sigma}_s^{-1}\mathbf{q}_k. \quad (12)$$

Then, we have [20]

$$\Delta\theta_k = -\frac{\lambda}{2\pi d \cos \theta_k} \Im\left(\frac{\Delta\mu_k}{\mu_k}\right), \quad (13)$$

where $\Im(\cdot)$ returns the imaginary part of a complex number. Unfortunately, this expression is “semi-algebraic” rather than explicit. In the following, we derive a closed-form MSE expression of the co-array-based standard ESPRIT method.

Proposition 1: The asymptotic second-order statistics of the estimation errors (in radians) by co-array-based standard ESPRIT is

$$\mathbb{E}(\Delta\theta_k^2) = \frac{\lambda^2 \mathbf{b}_k^H(\mathbf{R} \otimes \mathbf{R}^T)\mathbf{b}_k}{4\pi^2 d^2 \cos^2 \theta_k T}, \quad (14)$$

where

$$\begin{aligned} \mathbf{b}_k &= \mathbf{F}^T\mathbf{\Gamma}^T(\mathbf{h}_k \otimes \mathbf{g}_k), \quad \mathbf{h}_k = \mathbf{U}_s\mathbf{\Sigma}_s^{-1}\mathbf{q}_k \in \mathbb{C}^{\bar{N}_v \times 1}, \\ \mathbf{g}_k^T &= \mathbf{p}_k^T(\mathbf{J}_1\mathbf{U}_s)^\dagger(\mathbf{J}_2\mu_k^{-1} - \mathbf{J}_1)\mathbf{U}_n\mathbf{U}_n^H \in \mathbb{C}^{1 \times \bar{N}_v}. \end{aligned} \quad (15)$$

T is the number of snapshots.

Proof: Since $\text{vec}(\mathbf{A}\mathbf{X}\mathbf{B}) = (\mathbf{B}^T \otimes \mathbf{A})\text{vec}(\mathbf{X})$, we have

$$\begin{aligned} &\Im\left(\frac{\Delta\mu_k}{\mu_k}\right) \\ &= \Im\left[\mathbf{p}_k^T(\mathbf{J}_1\mathbf{U}_s)^\dagger(\mathbf{J}_2\mu_k^{-1} - \mathbf{J}_1)\mathbf{U}_n\mathbf{U}_n^H\Delta\mathbf{X}_v\mathbf{U}_s\mathbf{\Sigma}_s^{-1}\mathbf{q}_k\right], \\ &= \Im[(\mathbf{h}_k^T \otimes \mathbf{g}_k^T)\Delta\mathbf{x}_v] = \Im(\mathbf{b}_k^T\Delta\mathbf{r}), \end{aligned} \quad (16)$$

where $\Delta \mathbf{x}_v = \text{vec}(\Delta \mathbf{X}_v) = \mathbf{\Gamma} \mathbf{F} \Delta \mathbf{r}$. Then, calculating $\mathbb{E}[\Im^2(\mathbf{b}_k^T \Delta \mathbf{r})]$ yields

$$\mathbb{E}[\Im^2(\mathbf{b}_k^T \Delta \mathbf{r})] = \mathbb{E}[\Im(\mathbf{b}_k^T \Delta \mathbf{r}) \Im(\Delta \mathbf{r}^T \mathbf{b}_k)]$$

$$= \Re(\mathbf{b}_k^T) \mathbb{E}[\Im(\Delta \mathbf{r}) \Re(\Delta \mathbf{r}^T)] \Im(\mathbf{b}_k) + \quad (17a)$$

$$\Im(\mathbf{b}_k^T) \mathbb{E}[\Re(\Delta \mathbf{r}) \Re(\Delta \mathbf{r}^T)] \Im(\mathbf{b}_k) + \quad (17b)$$

$$\Re(\mathbf{b}_k^T) \mathbb{E}[\Im(\Delta \mathbf{r}) \Im(\Delta \mathbf{r}^T)] \Re(\mathbf{b}_k) + \quad (17c)$$

$$\Im(\mathbf{b}_k^T) \mathbb{E}[\Re(\Delta \mathbf{r}) \Im(\Delta \mathbf{r}^T)] \Re(\mathbf{b}_k), \quad (17d)$$

where $\Re(\cdot)$ returns the real part of a complex number. Next, we prove the structure of \mathbf{b}_k as follows.

Lemma 1: Let $\mathbf{B}_k = \text{mat}_{N_p, N_p}(\mathbf{b}_k)$, we have $j\mathbf{B}_k = (j\mathbf{B}_k)^H$, i.e., $\Re(\mathbf{B}_k^T) = -\Re(\mathbf{B}_k)$ and $\Im(\mathbf{B}_k^T) = \Im(\mathbf{B}_k)$.

Proof: According to [19, Lemma 3 and 6] and the property that $\text{vec}(\mathbf{a}\mathbf{b}^T) = \mathbf{b} \otimes \mathbf{a}$, we have

$$j\mathbf{B}_k = (j\mathbf{B}_k)^H \Leftrightarrow j\mathbf{h}_k \otimes \mathbf{g}_k = \Pi_{\bar{N}_v}^2(j\mathbf{h}_k \otimes \mathbf{g}_k)^*$$

$$\Leftrightarrow \mathbf{h}_k \mathbf{g}_k^T = -\Pi_{\bar{N}_v}(\mathbf{h}_k \mathbf{g}_k^T)^* \Pi_{\bar{N}_v}$$

$$\Leftrightarrow \mathbf{U}_s \Sigma_s^{-1} \mathbf{q}_k \mathbf{p}_k^T (\mathbf{J}_1 \mathbf{U}_s)^\dagger (\mathbf{J}_2 \mu_k^{-1} - \mathbf{J}_1) \mathbf{U}_n \mathbf{U}_n^H = \quad (18a)$$

$$-\Pi_{\bar{N}_v} [\mathbf{U}_s \Sigma_s^{-1} \mathbf{q}_k \mathbf{p}_k^T (\mathbf{J}_1 \mathbf{U}_s)^\dagger (\mathbf{J}_2 \mu_k^{-1} - \mathbf{J}_1) \mathbf{U}_n \mathbf{U}_n^H]^* \Pi_{\bar{N}_v}, \quad (18b)$$

where $\Pi_{\bar{N}_v}$ denotes the anti-identity matrix. The term in (18a) can be simplified to

$$\mathbf{U}_s \Sigma_s^{-1} \mathbf{q}_k \mathbf{p}_k^T (\mathbf{J}_1 \mathbf{U}_s)^\dagger (\mathbf{J}_2 \mu_k^{-1} - \mathbf{J}_1) (\mathbf{I} - \mathbf{U}_s \mathbf{U}_s^H)$$

$$= \mathbf{U}_s \Sigma_s^{-1} \mathbf{q}_k \mathbf{p}_k^T (\mathbf{J}_1 \mathbf{U}_s)^\dagger (\mathbf{J}_2 \mu_k^{-1} - \mathbf{J}_1) - \quad (19a)$$

$$\mathbf{U}_s \Sigma_s^{-1} \mathbf{q}_k \mathbf{p}_k^T (\Psi \mu_k^{-1} - \mathbf{I}) \mathbf{U}_s^H. \quad (19b)$$

According to the property of $\mathbf{p}_k^T \Psi = \mu_k \mathbf{p}_k^T$, we have $\mathbf{p}_k^T (\Psi \mu_k^{-1} - \mathbf{I}) = \mathbf{0}$. Then, the term in (19b) becomes zero. To prove the relationship in (18), it is necessary to check

$$\Pi_{\bar{N}_v} \mathbf{U}_s \Sigma_s^{-1} \mathbf{q}_k \mathbf{p}_k^T (\mathbf{J}_1 \mathbf{U}_s)^\dagger \mathbf{J}_2 \mu_k^{-1} \Pi_{\bar{N}_v} \quad (20a)$$

$$= [\mathbf{U}_s \Sigma_s^{-1} \mathbf{q}_k \mathbf{p}_k^T (\mathbf{J}_1 \mathbf{U}_s)^\dagger \mathbf{J}_1]^*. \quad (20b)$$

Since $\mu_k^{-1} = \mathbf{e}_k^T \Phi^{-1} \mathbf{e}_k$ (\mathbf{e}_k is the selection vector with its k -th element being 1 and others being 0), $\mathbf{U}_s \Sigma_s^{-1} \mathbf{U}_s^H = \mathbf{X}_{v0}^\dagger$ [18], $\mathbf{A}_v = \mathbf{U}_s \mathbf{T}$, $\mathbf{q}_k = \mathbf{T} \mathbf{e}_k$, $\mathbf{p}_k^T = \mathbf{e}_k^T \mathbf{T}^{-1}$ [17], and $(\mathbf{J}_1 \mathbf{U}_s)^\dagger = \mathbf{T}(\mathbf{J}_1 \mathbf{A}_v)^\dagger$ [22], the term in (20a) is updated to

$$\Pi_{\bar{N}_v} \mathbf{U}_s \Sigma_s^{-1} \mathbf{q}_k \mathbf{p}_k^T (\mathbf{J}_1 \mathbf{U}_s)^\dagger \mathbf{J}_2 \mu_k^{-1} \Pi_{\bar{N}_v}$$

$$= \Pi_{\bar{N}_v} \mathbf{U}_s \Sigma_s^{-1} \mathbf{U}_s^H \mathbf{A}_v \mathbf{e}_k \mathbf{e}_k^T \Phi^{-1} \mathbf{e}_k \mathbf{e}_k^T \mathbf{T}^{-1} \mathbf{T} (\mathbf{J}_1 \mathbf{A}_v)^\dagger \mathbf{J}_2 \Pi_{\bar{N}_v}$$

$$= \Pi_{\bar{N}_v} (\mathbf{A}_v^H)^\dagger \mathbf{P}^{-1} \mathbf{e}_k \mathbf{e}_k^T \Phi^{-1} (\mathbf{J}_1 \mathbf{A}_v)^\dagger \mathbf{J}_2 \Pi_{\bar{N}_v}. \quad (21)$$

Similarly, the term in (20b) is

$$[\mathbf{U}_s \Sigma_s^{-1} \mathbf{q}_k \mathbf{p}_k^T (\mathbf{J}_1 \mathbf{U}_s)^\dagger \mathbf{J}_1]^*$$

$$= [(\mathbf{A}_v^H)^\dagger \mathbf{P}^{-1} \mathbf{e}_k \mathbf{e}_k^T (\mathbf{J}_1 \mathbf{A}_v)^\dagger \mathbf{J}_1]^*. \quad (22)$$

Since $\Pi_{\bar{N}_v} \mathbf{A}_v = \mathbf{A}_v^* \Phi^{\bar{N}_v-1}$ [19], it is evident that

$$\Pi_{\bar{N}_v} \mathbf{A}_v (\mathbf{A}_v^H \mathbf{A}_v)^{-1} \mathbf{P}^{-1}$$

$$= \Pi_{\bar{N}_v} \mathbf{A}_v (\mathbf{A}_v^H \Pi_{\bar{N}_v} \Pi_{\bar{N}_v}^H \mathbf{A}_v)^{-1} \mathbf{P}^{-1} \quad (23)$$

$$= (\mathbf{A}_v^T)^\dagger \Phi^{\bar{N}_v-1} \mathbf{P}^{-1} = [(\mathbf{A}_v^H)^\dagger \mathbf{P}^{-1}]^* \Phi^{\bar{N}_v-1}.$$

The relationship in (20) is satisfied if

$$\Phi^{\bar{N}_v-2} (\mathbf{J}_1 \mathbf{A}_v)^\dagger \mathbf{J}_2 \Pi_{\bar{N}_v} = [(\mathbf{J}_1 \mathbf{A}_v)^\dagger \mathbf{J}_1]^*$$

$$\Leftrightarrow \Phi^{\bar{N}_v-2} (\mathbf{J}_1 \mathbf{A}_v)^\dagger \Pi_{\bar{N}_v-1} = [(\mathbf{J}_1 \mathbf{A}_v)^\dagger]^*. \quad (24)$$

Based on $\Pi_{\bar{N}_v-1} \mathbf{A}_{v1} = \mathbf{A}_{v1}^* \Phi^{\bar{N}_v-2} (\mathbf{J}_1 \mathbf{A}_v = \mathbf{A}_{v1})$, we have

$$\Phi^{\bar{N}_v-2} (\mathbf{A}_{v1}^H \Pi_{\bar{N}_v-1} \Pi_{\bar{N}_v-1}^H \mathbf{A}_{v1})^{-1} \mathbf{A}_{v1}^H \Pi_{\bar{N}_v-1}$$

$$= \Phi^{\bar{N}_v-2} (\Phi^{2-\bar{N}_v} \mathbf{A}_{v1}^T \mathbf{A}_{v1}^* \Phi^{\bar{N}_v-2})^{-1} \Phi^{2-\bar{N}_v} \mathbf{A}_{v1}^T \quad (25)$$

$$= (\mathbf{A}_{v1}^\dagger)^* = [(\mathbf{J}_1 \mathbf{A}_v)^\dagger]^*,$$

which completes the proof of Lemma 1. \blacksquare

According to [19, Lemma 3] and [19, Lemma 4], the term in (17a) becomes

$$\Re(\mathbf{b}_k^T) \mathbb{E}[\Im(\Delta \mathbf{r}) \Re(\Delta \mathbf{r}^T)] \Im(\mathbf{b}_k)$$

$$= \frac{1}{2T} \Re(\mathbf{b}_k^T) \left[\Re(\mathbf{R}) \otimes \Im(\mathbf{R}) - \Im(\mathbf{R}) \otimes \Re(\mathbf{R}) \right] \Im(\mathbf{b}_k) -$$

$$\frac{1}{2T} \Re(\mathbf{b}_k^T) \left[\Im(\mathbf{R}) \otimes \Re(\mathbf{R}) - \Re(\mathbf{R}) \otimes \Im(\mathbf{R}) \right] \Im(\mathbf{b}_k)$$

$$= \frac{1}{T} \Re(\mathbf{b}_k^T) \Im(\mathbf{R}^T \otimes \mathbf{R}) \Im(\mathbf{b}_k), \quad (26)$$

where $\mathbf{W}(\mathbf{A}, \mathbf{B})$ is defined as [19, Definition 2]

$$\mathbf{W}(\mathbf{A}, \mathbf{B}) = \begin{bmatrix} \mathbf{a}_1 \mathbf{b}_1^T & \cdots & \mathbf{a}_N \mathbf{b}_1^T \\ \vdots & \ddots & \vdots \\ \mathbf{a}_1 \mathbf{b}_N^T & \cdots & \mathbf{a}_N \mathbf{b}_N^T \end{bmatrix}, \quad (27)$$

with $\mathbf{A} = [\mathbf{a}_1, \dots, \mathbf{a}_N] \in \mathbb{R}^{N \times N}$ and $\mathbf{B} = [\mathbf{b}_1, \dots, \mathbf{b}_N] \in \mathbb{R}^{N \times N}$. Similar for other terms in (17b), (17c), and (17d), finally we obtain

$$\mathbb{E}[\Im^2(\mathbf{b}_k^T \Delta \mathbf{r})] = \frac{\mathbf{b}_k^H (\mathbf{R} \otimes \mathbf{R}^T) \mathbf{b}_k}{T}. \quad (28)$$

Substituting (16) and (28) into (13) completes the proof of Proposition 1. \blacksquare

B. Performance Analysis of Co-Array-Based Unitary ESPRIT

The unitary pre-processing technique involved in the unitary ESPRIT method leads to complexity reduction. The symbol (\cdot) is used to represent the unitary pre-processed (forward-backward averaging) version of an input variable [5], [21], e.g.,

$$\tilde{\mathbf{X}}_v = [\Re(\mathbf{Q}_{\bar{N}_v}^H \mathbf{X}_v), \Im(\mathbf{Q}_{\bar{N}_v}^H \mathbf{X}_v)]. \quad (29)$$

Here, for $\bar{N}_v = 2P$,

$$\mathbf{Q}_{2P} = \frac{1}{\sqrt{2}} \begin{bmatrix} \mathbf{I}_P & j\mathbf{I}_P \\ \mathbf{\Pi}_P & -j\mathbf{\Pi}_P \end{bmatrix}, \quad (30)$$

while for $\bar{N}_v = 2P + 1$,

$$\mathbf{Q}_{2P+1} = \frac{1}{\sqrt{2}} \begin{bmatrix} \mathbf{I}_P & \mathbf{0}_P & j\mathbf{I}_P \\ \mathbf{0}_P^T & \sqrt{2} & \mathbf{0}_P^T \\ \mathbf{\Pi}_P & \mathbf{0}_P & -j\mathbf{\Pi}_P \end{bmatrix}. \quad (31)$$

Correspondingly, the rotation invariance selection matrices are $\tilde{\mathbf{J}}_1 = \Re(\mathbf{Q}_{\bar{N}_v-1}^H \mathbf{J}_2 \mathbf{Q}_{\bar{N}_v})$ and $\tilde{\mathbf{J}}_2 = \Im(\mathbf{Q}_{\bar{N}_v-1}^H \mathbf{J}_2 \mathbf{Q}_{\bar{N}_v})$, and $\tilde{\Phi} = \text{diag}([\tilde{\mu}_1, \dots, \tilde{\mu}_K])$ holds information related to DOAs with $\tilde{\mu}_k = \tan(-\frac{\pi}{\lambda} d \sin \theta_k)$.

Proposition 2: The asymptotic MSE of DOA estimation by co-array-based UESPRIT method is

$$\mathbb{E}(\Delta\theta_k^2) = \frac{4\lambda^2 \mathbf{c}_k^H (\mathbf{R} \otimes \mathbf{R}^T) \mathbf{c}_k}{\pi^2 d^2 \cos^2 \theta_k T (1 + \tilde{\mu}_k^2)^2}, \quad (32)$$

with

$$\begin{aligned} \mathbf{c}_k &= \mathbf{K}^T (\tilde{\mathbf{b}}_{1k} - j\tilde{\mathbf{b}}_{2k}), \quad \mathbf{K} = \frac{1}{2} (\mathbf{I} \otimes \mathbf{Q}_{N_v}^H) \mathbf{\Gamma} \mathbf{F}, \\ \tilde{\mathbf{b}}_k &= \tilde{\mathbf{h}}_k \otimes \tilde{\mathbf{g}}_k = [\tilde{\mathbf{b}}_{1k}^T, \tilde{\mathbf{b}}_{2k}^T]^T, \quad \tilde{\mathbf{h}}_k = \tilde{\mathbf{V}}_s \tilde{\Sigma}_s^{-1} \tilde{\mathbf{q}}_k \in \mathbb{R}^{2N_v \times 1}, \\ \tilde{\mathbf{g}}_k^T &= \tilde{\mathbf{p}}_k^T (\tilde{\mathbf{J}}_1 \tilde{\mathbf{U}}_s)^\dagger (\tilde{\mathbf{J}}_2 - \tilde{\mu}_k \tilde{\mathbf{J}}_1) \tilde{\mathbf{U}}_n \tilde{\mathbf{U}}_n^H \in \mathbb{R}^{1 \times N_v}, \end{aligned}$$

where $\tilde{\mathbf{b}}_{1k}, \tilde{\mathbf{b}}_{2k} \in \mathbb{R}^{N_v \times 1}$ and $\tilde{\mathbf{b}}_k = [\tilde{\mathbf{b}}_{1k}^T, \tilde{\mathbf{b}}_{2k}^T]^T$.

Proof: Recalling (12), the perturbation of the unitary version eigenvalue is

$$\begin{aligned} \Delta\tilde{\mu}_k &= \tilde{\mathbf{p}}_k^T (\tilde{\mathbf{J}}_1 \tilde{\mathbf{U}}_s)^\dagger (\tilde{\mathbf{J}}_2 - \tilde{\mu}_k \tilde{\mathbf{J}}_1) \tilde{\mathbf{U}}_n \tilde{\mathbf{U}}_n^H \Delta\tilde{\mathbf{X}}_v \tilde{\mathbf{V}}_s \tilde{\Sigma}_s^{-1} \tilde{\mathbf{q}}_k \\ &= \tilde{\mathbf{g}}_k^T \Delta\tilde{\mathbf{X}}_v \tilde{\mathbf{h}}_k = (\tilde{\mathbf{h}}_k^T \otimes \tilde{\mathbf{g}}_k^T) \Delta\tilde{\mathbf{x}}_v = \tilde{\mathbf{b}}_k^T \Delta\tilde{\mathbf{x}}_v. \end{aligned} \quad (33)$$

According to (29) and $\text{vec}(\mathbf{AXB}) = (\mathbf{B}^T \otimes \mathbf{A}) \text{vec}(\mathbf{X})$, we have

$$\begin{aligned} \Delta\tilde{\mathbf{x}}_v &= \begin{bmatrix} \frac{1}{2} \text{vec}(\mathbf{Q}_{N_v}^H \Delta\mathbf{X}_v) + \frac{1}{2} \text{vec}(\mathbf{Q}_{N_v}^T \Delta\mathbf{X}_v^*) \\ \frac{1}{2j} \text{vec}(\mathbf{Q}_{N_v}^H \Delta\mathbf{X}_v) - \frac{1}{2j} \text{vec}(\mathbf{Q}_{N_v}^T \Delta\mathbf{X}_v^*) \end{bmatrix} \\ &= \begin{bmatrix} \frac{1}{2} (\mathbf{I} \otimes \mathbf{Q}_{N_v}^H) \mathbf{\Gamma} \mathbf{F} \Delta\mathbf{r} + \frac{1}{2} (\mathbf{I} \otimes \mathbf{Q}_{N_v}^T) \mathbf{\Gamma} \mathbf{F} \Delta\mathbf{r}^* \\ \frac{1}{2j} (\mathbf{I} \otimes \mathbf{Q}_{N_v}^H) \mathbf{\Gamma} \mathbf{F} \Delta\mathbf{r} - \frac{1}{2j} (\mathbf{I} \otimes \mathbf{Q}_{N_v}^T) \mathbf{\Gamma} \mathbf{F} \Delta\mathbf{r}^* \end{bmatrix} \\ &= \begin{bmatrix} \mathbf{K} \Delta\mathbf{r} + \mathbf{K}^* \Delta\mathbf{r}^* \\ -j\mathbf{K} \Delta\mathbf{r} + j\mathbf{K}^* \Delta\mathbf{r}^* \end{bmatrix}. \end{aligned} \quad (34)$$

Substituting (34) into (33) yields

$$\begin{aligned} \Delta\tilde{\mu}_k &= [\tilde{\mathbf{b}}_{1k}^T, \tilde{\mathbf{b}}_{2k}^T] \begin{bmatrix} \mathbf{K} \Delta\mathbf{r} + \mathbf{K}^* \Delta\mathbf{r}^* \\ -j\mathbf{K} \Delta\mathbf{r} + j\mathbf{K}^* \Delta\mathbf{r}^* \end{bmatrix} \\ &= (\tilde{\mathbf{b}}_{1k}^T - j\tilde{\mathbf{b}}_{2k}^T) \mathbf{K} \Delta\mathbf{r} + (\tilde{\mathbf{b}}_{1k}^T + j\tilde{\mathbf{b}}_{2k}^T) \mathbf{K}^* \Delta\mathbf{r}^* \\ &= 2\Re(\mathbf{c}_k^T \Delta\mathbf{r}). \end{aligned} \quad (35)$$

For \mathbf{c}_k , the following Lemma holds true.

Lemma 2: With $\mathbf{C}_k = \text{mat}_{N_p, N_p}(\mathbf{c}_k)$, there is $\mathbf{C}_k = \mathbf{C}_k^H$.

Proof: Following a similar process as that in [19, Lemma 4], the necessary condition of the lemma is

$$\begin{aligned} \mathbf{Q}_{N_v}^* \tilde{\mathbf{g}}_k (\tilde{\mathbf{h}}_{1k}^T - j\tilde{\mathbf{h}}_{2k}^T) &= \Pi_{N_v} [\mathbf{Q}_{N_v}^* \tilde{\mathbf{g}}_k (\tilde{\mathbf{h}}_{1k}^T - j\tilde{\mathbf{h}}_{2k}^T)]^* \Pi_{N_v} \\ &\Leftrightarrow (\tilde{\mathbf{V}}_{s1} - j\tilde{\mathbf{V}}_{s2}) \tilde{\Sigma}_s^{-1} \tilde{\mathbf{q}}_k \tilde{\mathbf{p}}_k^T (\tilde{\mathbf{J}}_1 \tilde{\mathbf{U}}_s)^\dagger (\tilde{\mathbf{J}}_2 - \tilde{\mu}_k \tilde{\mathbf{J}}_1) \tilde{\mathbf{U}}_n \tilde{\mathbf{U}}_n^H \mathbf{Q}_{N_v}^H = \end{aligned} \quad (36a)$$

$$\begin{aligned} \Pi_{N_v} [(\tilde{\mathbf{V}}_{s1} - j\tilde{\mathbf{V}}_{s2}) \tilde{\Sigma}_s^{-1} \tilde{\mathbf{q}}_k \tilde{\mathbf{p}}_k^T (\tilde{\mathbf{J}}_1 \tilde{\mathbf{U}}_s)^\dagger (\tilde{\mathbf{J}}_2 - \tilde{\mu}_k \tilde{\mathbf{J}}_1) \tilde{\mathbf{U}}_n \tilde{\mathbf{U}}_n^H \mathbf{Q}_{N_v}^H] &= \Pi_{N_v} [(\tilde{\mathbf{V}}_{s1} - j\tilde{\mathbf{V}}_{s2}) \tilde{\Sigma}_s^{-1} \tilde{\mathbf{q}}_k \tilde{\mathbf{p}}_k^T (\tilde{\mathbf{J}}_1 \tilde{\mathbf{U}}_s)^\dagger (\tilde{\mathbf{J}}_2 - \tilde{\mu}_k \tilde{\mathbf{J}}_1) \tilde{\mathbf{U}}_n \tilde{\mathbf{U}}_n^H \mathbf{Q}_{N_v}^H] \\ &= \tilde{\mu}_k \tilde{\mathbf{J}}_1 \tilde{\mathbf{U}}_n \tilde{\mathbf{U}}_n^H \mathbf{Q}_{N_v}^H \Pi_{N_v}, \end{aligned} \quad (36b)$$

where $\tilde{\mathbf{h}}_{1k}, \tilde{\mathbf{h}}_{2k} \in \mathbb{R}^{N_v \times 1}$ and $\tilde{\mathbf{h}}_k = [\tilde{\mathbf{h}}_{1k}, \tilde{\mathbf{h}}_{2k}]$, $\tilde{\mathbf{V}}_{s1}, \tilde{\mathbf{V}}_{s2} \in \mathbb{R}^{N_v \times K}$. Since $(\tilde{\mathbf{V}}_{s1} - j\tilde{\mathbf{V}}_{s2}) \tilde{\Sigma}_s^{-1} \tilde{\mathbf{U}}_s = (\mathbf{Q}_{N_v}^H \mathbf{X}_{v0})^\dagger$, $\mathbf{Q}_{N_v}^H \mathbf{A}_v = \tilde{\mathbf{U}}_s \tilde{\mathbf{T}}$, $\tilde{\mathbf{q}}_k = \tilde{\mathbf{T}} \mathbf{e}_k$, $\tilde{\mathbf{p}}_k^T = \mathbf{e}_k^T \tilde{\mathbf{T}}^{-1}$, $(\tilde{\mathbf{J}}_1 \tilde{\mathbf{U}}_s)^\dagger =$

$\tilde{\mathbf{T}}(\tilde{\mathbf{J}}_1 \mathbf{Q}_{N_v}^H \mathbf{A}_v)^\dagger$, and $\tilde{\mathbf{p}}_k^T (\tilde{\mathbf{V}} \tilde{\mu}_k^{-1} - \mathbf{I}) = \mathbf{0}$, the term in (36a) is simplified to

$$\begin{aligned} &(\tilde{\mathbf{V}}_{s1} - j\tilde{\mathbf{V}}_{s2}) \tilde{\Sigma}_s^{-1} \tilde{\mathbf{q}}_k \tilde{\mathbf{p}}_k^T (\tilde{\mathbf{J}}_1 \tilde{\mathbf{U}}_s)^\dagger (\tilde{\mathbf{J}}_2 - \tilde{\mu}_k \tilde{\mathbf{J}}_1) \tilde{\mathbf{U}}_n \tilde{\mathbf{U}}_n^H \mathbf{Q}_{N_v}^H \\ &= (\mathbf{Q}_{N_v}^H \mathbf{X}_{v0})^\dagger \mathbf{Q}_{N_v}^H \mathbf{A}_v \mathbf{e}_k \mathbf{e}_k^T \tilde{\mathbf{T}}^{-1} \tilde{\mathbf{T}} (\tilde{\mathbf{J}}_1 \mathbf{Q}_{N_v}^H \mathbf{A}_v)^\dagger \\ &\quad (\tilde{\mathbf{J}}_2 - \tilde{\mu}_k \tilde{\mathbf{J}}_1) \mathbf{Q}_{N_v}^H \\ &= (\mathbf{A}_v^H)^\dagger \mathbf{P}^{-1} \mathbf{e}_k \mathbf{e}_k^T (\tilde{\mathbf{J}}_1 \mathbf{Q}_{N_v}^H \mathbf{A}_v)^\dagger (\tilde{\mathbf{J}}_2 - \tilde{\mu}_k \tilde{\mathbf{J}}_1) \mathbf{Q}_{N_v}^H. \end{aligned} \quad (37)$$

and the term in (36b) can be simplified similarly. It is equivalent to proving the following two equations:

$$\Phi^{\bar{N}_v-1} (\tilde{\mathbf{J}}_1 \mathbf{Q}_{N_v}^H \mathbf{A}_v)^\dagger \tilde{\mathbf{J}}_1 \mathbf{Q}_{N_v}^H \Pi_{N_v} = [(\tilde{\mathbf{J}}_1 \mathbf{Q}_{N_v}^H \mathbf{A}_v)^\dagger \tilde{\mathbf{J}}_1 \mathbf{Q}_{N_v}^H]^* \quad (38)$$

and

$$\Phi^{\bar{N}_v-1} (\tilde{\mathbf{J}}_1 \mathbf{Q}_{N_v}^H \mathbf{A}_v)^\dagger \tilde{\mathbf{J}}_2 \mathbf{Q}_{N_v}^H \Pi_{N_v} = [(\tilde{\mathbf{J}}_1 \mathbf{Q}_{N_v}^H \mathbf{A}_v)^\dagger \tilde{\mathbf{J}}_2 \mathbf{Q}_{N_v}^H]^*. \quad (39)$$

Since $\mathbf{Q}_{N_v}^H \Pi_{N_v} = \mathbf{Q}_{N_v}^T$, we only need to prove that

$$\Phi^{\bar{N}_v-1} (\tilde{\mathbf{J}}_1 \mathbf{Q}_{N_v}^H \mathbf{A}_v)^\dagger = [(\tilde{\mathbf{J}}_1 \mathbf{Q}_{N_v}^H \mathbf{A}_v)^\dagger]^*. \quad (40)$$

Then, with $\tilde{\mathbf{J}}_1 \mathbf{Q}_{N_v}^H = \frac{1}{2} \mathbf{Q}_{N_v-1}^H (\mathbf{J}_1 + \mathbf{J}_2)$, we have

$$\begin{aligned} &\Phi^{\bar{N}_v-1} (\mathbf{Q}_{N_v-1}^H \mathbf{A}_{v1})^\dagger = [(\mathbf{Q}_{N_v-1}^H \mathbf{A}_{v2})^\dagger]^* \\ &\Leftrightarrow \Phi [(\mathbf{A}_{v1}^H \mathbf{A}_{v1})^{-1} \mathbf{A}_{v1}^H] \Pi_{N_v-1} \mathbf{Q}_{N_v-1} \\ &\quad = [(\mathbf{A}_{v2}^H \mathbf{A}_{v2})^{-1} \mathbf{A}_{v2}^H \mathbf{Q}_{N_v-1}]^* \\ &\Leftrightarrow \Phi (\mathbf{A}_{v1}^\dagger)^* = (\mathbf{A}_{v2}^\dagger)^* \Leftrightarrow \mathbf{A}_{v1} \Phi = \mathbf{A}_{v2}, \end{aligned} \quad (41)$$

which completes the proof of Lemma 2. ■

Following a similar process in obtaining (26), the MSE of eigenvalue is $\mathbb{E}(\Delta\tilde{\mu}_k^2) = \frac{4}{T} \Re[\mathbf{c}_k^H (\mathbf{R} \otimes \mathbf{R}^T) \mathbf{c}_k]$. With the relationship of $\tilde{\mu}_k = \tan(-\frac{\pi d}{\lambda} \sin \theta_k)$, we can derive that

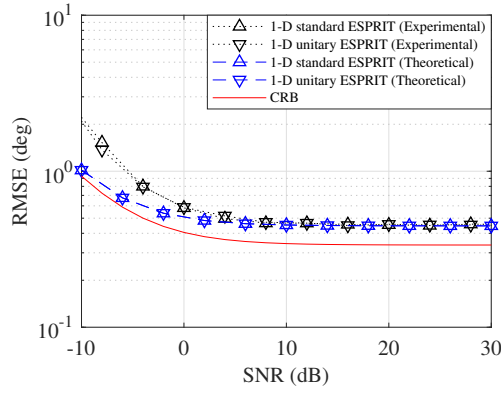
$$\mathbb{E}(\Delta\theta_k^2) = \frac{\lambda^2 \mathbb{E}(\Delta\tilde{\mu}_k^2)}{\pi^2 d^2 \cos^2 \theta_k T (1 + \tilde{\mu}_k^2)^2}, \quad (42)$$

which completes the proof of Proposition 2. ■

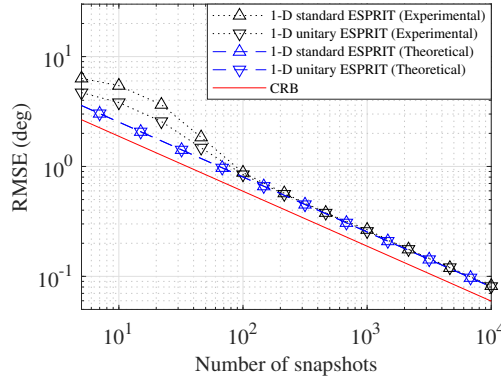
IV. SIMULATION RESULTS

In this section, the experimental root mean square error (RMSE) results of ESPRIT-type methods (including co-array-based standard ESPRIT method and co-array-based unitary ESPRIT method) via Monte Carlo simulations with 1000 trials are compared with the derived asymptotic theoretical performance bounds ((14) and (32)) and also CRBs [19]. The nested array with 6 sensors is considered with sensors located at $\{0, 1, 2, 3, 7, 11\}d$, and the unit inter-element spacing is $d = \frac{\lambda}{2}$. The underdetermined case is examined with $K = 9$ sources uniformly distributed within $\theta \in [-60^\circ, 60^\circ]$, and the sensor number exceeds the number of physical sensors.

The MSE results versus input SNR are shown in Fig. 1(a) with the number of snapshots set to $T = 300$. It is observed that the experimental RMSE results converge to our theoretical performance bounds for SNR larger than 5 dB. The CRB



(a) RMSE versus SNR.



(b) RMSE versus the number of snapshots.

Fig. 1. Experimental and theoretical asymptotic RMSE results of co-array-based ESPRIT-type methods.

is lower than both the experimental and theoretical results, indicating that the derived explicit performance bounds are sufficiently tight to evaluate the DOA estimation performance of corresponding methods.

Then in Fig. 1(b), the MSE results with respect to the number of snapshots are included with SNR fixed at 10 dB. Clearly, the empirical RMSE results approximate the theoretical performance bounds for $T \geq 100$, and the derived explicit bounds are more suitable as performance evaluation tools.

V. CONCLUSION

In this paper, the performance for DOA estimation of ESPRIT-type methods was analyzed. The co-array-based standard ESPRIT method was first considered with closed-form expression of its performance bound for DOA estimation derived. Then, we focused on the co-array-based unitary ESPRIT method, and derived an explicit asymptotic performance bound. As verified by simulations, existing CRB is loose for evaluation of ESPRIT-type methods, while the derived bounds are tight and effective.

REFERENCES

- [1] H. L. V. Trees, *Optimum Array Processing: Part IV of Detection, Estimation, and Modulation Theory*. John Wiley & Sons, Ltd, 2002.
- [2] R. Schmidt, "Multiple emitter location and signal parameter estimation," *IEEE Transactions on Antennas and Propagation*, vol. 34, no. 3, pp. 276–280, 1986.
- [3] A. Barabell, "Improving the resolution performance of eigenstructure-based direction-finding algorithms," in *Proc. IEEE International Conference on Acoustics, Speech, and Signal Processing*, vol. 8, 1983, pp. 336–339.
- [4] R. Roy, A. Paulraj, and T. Kailath, "ESPRIT—a subspace rotation approach to estimation of parameters of cisoids in noise," *IEEE Transactions on Acoustics, Speech, and Signal Processing*, vol. 34, no. 5, pp. 1340–1342, 1986.
- [5] M. Haardt and J. Nossek, "Unitary ESPRIT: how to obtain increased estimation accuracy with a reduced computational burden," *IEEE Transactions on Signal Processing*, vol. 43, no. 5, pp. 1232–1242, 1995.
- [6] Q. Shen, W. Liu, W. Cui, and S. Wu, "Underdetermined DOA estimation under the compressive sensing framework: A review," *IEEE Access*, vol. 4, pp. 8865–8878, 2016.
- [7] P. Pal and P. Vaidyanathan, "Nested arrays: A novel approach to array processing with enhanced degrees of freedom," *IEEE Transactions on Signal Processing*, vol. 58, pp. 4167–4181, 09 2010.
- [8] Q. Shen, W. Liu, W. Cui, and S. Wu, "Extension of co-prime arrays based on the fourth-order difference co-array concept," *IEEE Signal Processing Letters*, vol. 23, no. 5, pp. 615–619, May 2016.
- [9] Q. Shen, W. Liu, W. Cui, S. Wu, and P. Pal, "Simplified and enhanced multiple level nested arrays exploiting high-order difference co-arrays," *IEEE Transactions on Signal Processing*, vol. 67, no. 13, pp. 3502–3515, Jul. 2019.
- [10] P. Pal and P. P. Vaidyanathan, "Coprime sampling and the MUSIC algorithm," in *Proc. Digital Signal Processing and Signal Processing Education Meeting (DSP/SPE)*, 2011, pp. 289–294.
- [11] P. Pal and P. Vaidyanathan, "Nested arrays in two dimensions, part I: Geometrical considerations," *IEEE Transactions on Signal Processing*, vol. 60, pp. 4694–4705, 09 2012.
- [12] C.-L. Liu and P. P. Vaidyanathan, "Hourglass arrays and other novel 2-D sparse arrays with reduced mutual coupling," *IEEE Transactions on Signal Processing*, vol. 65, no. 13, pp. 3369–3383, 2017.
- [13] S. Ren, X. Li, X. Luo, and W. Wang, "Extensions of open box array with reduced mutual coupling," *IEEE Sensors Journal*, vol. 18, no. 13, pp. 5475–5484, 2018.
- [14] Z. Yang, Q. Shen, W. Liu, Y. C. Eldar, and W. Cui, "High-order cumulants based sparse array design via fractal geometries—part I: Structures and dofs," *IEEE Transactions on Signal Processing*, vol. 71, pp. 327–342, 2023.
- [15] —, "High-order cumulants based sparse array design via fractal geometries—part II: Robustness and mutual coupling," *IEEE Transactions on Signal Processing*, vol. 71, pp. 343–357, 2023.
- [16] Q. Shen, W. Liu, W. Cui, S. Wu, Y. D. Zhang, and M. G. Amin, "Low-complexity direction-of-arrival estimation based on wideband co-prime arrays," *IEEE/ACM Transactions on Audio, Speech, and Language Processing*, vol. 23, no. 9, pp. 1445–1456, 2015.
- [17] F. Li, H. Liu, and R. Vaccaro, "Performance analysis for DOA estimation algorithms: unification, simplification, and observations," *IEEE Transactions on Aerospace and Electronic Systems*, vol. 29, pp. 1170 – 1184, 11 1993.
- [18] B. Rao and K. Hari, "Performance analysis of ESPRIT and TAM in determining the direction of arrival of plane waves in noise," *IEEE Transactions on Acoustics, Speech, and Signal Processing*, vol. 37, no. 12, pp. 1990–1995, 1989.
- [19] M. Wang and A. Nehorai, "Coarrays, MUSIC, and the Cramér-Rao bound," *IEEE Transactions on Signal Processing*, vol. 65, no. 4, pp. 933–946, 2017.
- [20] J. Steinwandt, F. Roemer, and M. Haardt, "Performance analysis of ESPRIT-type algorithms for co-array structures," in *Proc. IEEE International Workshop on Computational Advances in Multi-Sensor Adaptive Processing (CAMSAP)*, 2017, pp. 1–5.
- [21] M. Zoltowski, M. Haardt, and C. Mathews, "Closed-form 2-D angle estimation with rectangular arrays in element space or beamspace via unitary ESPRIT," *IEEE Transactions on Signal Processing*, vol. 44, no. 2, pp. 316–328, 1996.
- [22] K. B. Petersen, M. S. Pedersen *et al.*, "The matrix cookbook," *Technical University of Denmark*, vol. 7, no. 15, p. 510, 2008.